HHS Public Access

Author manuscript

Cell Microbiol. Author manuscript; available in PMC 2022 February 01.

Published in final edited form as:

Cell Microbiol. 2021 February ; 23(2): e13281. doi:10.1111/cmi.13281.

MicroRNA-206 inhibits influenza A virus replication by targeting tankyrase 2

Gayan Bamunuarachchi[1,2], **Xiaoyun Yang**[1,2], **Chaoqun Huang**[1,2], **Yurong Liang**[1,2], **Yujie Guo**, **Lin Liu**[1,2]

[1]Oklahoma Center for Respiratory and Infectious Diseases, Oklahoma State University, Stillwater, Oklahoma

[2]Lundberg-Kienlen Lung Biology and Toxicology Laboratory, Department of Physiological Sciences, Oklahoma State University, Stillwater, Oklahoma

Abstract

Due to the frequent mutations, influenza A virus (IAV) becomes resistant to anti-viral drugs targeting influenza viral proteins. There are increasing interests in anti-viral agents that target host cellular proteins required for virus replication. Tankyrase (TNKS) has poly (ADP-ribose) polymerase activity and is a negative regulator of many host proteins. The objectives of this study are to study the role of TNKS2 in IAV infection, identify the microRNAs targeting TNKS2, and to understand the mechanisms involved. We found that TNKS2 expression was elevated in human lung epithelial cells and mouse lungs during IAV infection. Knock-down of TNKS2 by RNA interference reduced viral replication. Using a computation approach and 3'-untranslation regions (3'-UTR) reporter assay, we identified miR-206 as the micro-RNA that targeted TNKS2. Overexpression of miR-206 reduced viral protein levels and virus production in cell culture. The effect of miR-206 on IAV replication was strain-independent. miR-206 activated JNK/c-Jun signalling, induced type I interferon expression and enhanced Stat signalling. Finally, the delivery of an adenovirus expressing miR-206 into the lung of mice challenged with IAV increased type I interferon response, suppressed viral load in the lungs and increased survival. Our results indicate that miR-206 has anti-influenza activity by targeting TNKS2 and subsequently activating the anti-viral sate.

Correspondence: Lin Liu, Department of Physiological Sciences, OklahomaState University, 264 McElroy Hall, Stillwater, OK 74078, USA. lin.liu@okstate.edu.

AUTHORS CONTRIBUTION

Gayan Bamunuarachchi performed experiments, analysed data, and wrote the manuscript. Xiaoyun Yang, Chaoqun Huang, Yurong Liang, and Yujie Guo performed experiments and analysed data. Lin Liu designed the concept of the paper, provided resources, analysed data, and wrote the manuscript.

DATA AVAILABILITY STATEMENT

Data sharing not applicable to this article as no datasets were generated or analyzed during the current study.

CONFLICT OF INTEREST

The authors declare no conflicts of interest.

SUPPORTING INFORMATION

Additional supporting information may be found online in the supporting information section at the end of this article.

1 | INTRODUCTION

The influenza virus belongs to the *Orthomyxoviridae* family and is one of the most common causes of human respiratory infections. There is evidence that influenza outbreaks have occurred since ancient times (Taubenberger & Kash, 2010). Seasonal influenza-associated deaths in the US ranged from a low of 12,000 (during 2011–2012) to a high of 61,000 (during 2017–2018) (Center of Disease Control, 2020, April 17). In addition to annual winter outbreaks, unpredictable pandemic influenza viruses emerge every 8–41 years for the past several centuries (Taubenberger & Kash, 2010). Influenza virus can lead to a higher mortality rate when the elderly, infants and people with chronic diseases are infected.

The influenza virus is a single-stranded, eight-segmented, and negative-sense RNA virus. Its genome replication is dependent on RNA-dependent RNA polymerase of viral origin and is error-prone. This can cause frequent mutations and changes in the viral genome and protein structure, which enable the virus to evade the host immune system (Bouvier & Palese, 2008; van de Sandt, Kreijtz, & Rimmelzwaan, 2012). Vaccination is an effective and long-lasting method to prevent influenza virus infection. However, there are several limitations including the requirement of annual updates, relatively long production times, moderate efficacy in certain populations, limited vaccine capacity and lack of cross-reactivity (Soema, Kompier, Amorij, & Kersten, 2015). Anti-viral drugs are another choice of treatment. Current anti-influenza drugs target viral proteins and the influenza virus becomes to resist to these drugs due to its high mutation rate (Hussain, Galvin, Haw, Nutsford, & Husain, 2017). The development of new anti-influenza drugs that are effective regardless of virus changes is a critical need. Since the influenza virus needs many host factors to complete its replication cycle (Konig et al., 2010), targeting host factors may influence the pathology and the progression of infection and thus is a promising approach for developing influenza therapeutics.

Tankyrase (TNKS), first discovered in 1998 consists of two isoforms, TNKS1 and TNKS2. They are members of the poly (ADP-ribose) polymerase (PARP) superfamily. TNKS1 is encoded by the *TNKS1* gene on human chromosome 8 and contains four distinct domains: an amino-terminal histidine, proline and serine rich (HPS) domain, an ankyrin domain, a sterile alpha module (SAM) domain and a carboxyl-terminal PARP catalytic domain (Riffell, Lord, & Ashworth, 2012). TNKS2 is encoded by the *TNKS2* gene on human chromosome 10 and shares 81% nucleotide homology and a similar intracellular distribution pattern with TNKS1 (Qiu et al., 2014). However, TNKS2 lacks HPS domain (Kaminker et al., 2001). TNKS is implicated in many biological processes such as cancer progression, regulation of telomere length, lung fibrogenesis and myelination (Riffell et al., 2012). TNKS is also involved in virus infection. While TNKS inhibits Epstein–Barr virus OriP function and subsequent replication in a PARP-dependent manner (Deng et al., 2005), TNKS inhibitor XAV939 reduces replication of herpes simplex virus (Z. Li et al., 2012). Additionally, human cytomegalovirus inhibits TNKS activity (Roy, Liu, & Arav-Boger, 2016). However, whether TNKS regulates influenza virus replication is unclear.

MicroRNA (miRNAs) are small (~22 nt) noncoding endogenous RNAs that regulate the expression of many protein-coding genes. miRNAs target specific mRNAs through

complementary binding sites in their 3'-untranslated (3'-UTR) region. This binding leads to either mRNA degradation or translation inhibition (Bartel, 2004). miRNAs are functionally linked to numerous diseases. Cellular miRNAs regulate innate immunity associated with diseases of viral origin and play a critical role in the pathology of several respiratory viruses (Umbach & Cullen, 2009; L. Zhao et al., 2015). Influenza virus alters the expression of host miRNAs (Gui et al., 2015; Ingle et al., 2015; L. Zhao et al., 2015). On the other hand, miRNAs regulate influenza virus infection. Some miRNAs such as miR-323, miR-491, and miR-654 inhibit the replication of the H1N1 IAV by targeting the conserved regions in viral polymerase gene PB1 (Song, Liu, Gao, Jiang, & Huang, 2010). Other miRNAs including miR-136, miR-485, miR-302c, and miR-193b attenuate IAV replication by regulating host factors (Gui et al., 2015; Ingle et al., 2015; X. Yang et al., 2019; L. Zhao et al., 2015).

Human miR-206 is located on chromosome 6 and has a highly conserved sequence among vertebrates (G. Ma et al., 2015). Dysregulation of miR-206 is linked to various diseases including heart failure, chronic obstructive pulmonary disease, Alzheimer's disease and various types of cancers (Novak, Kruzliak, Bienertova-Vasku, Slaby, & Novak, 2014). miR-206 also suppresses the replication of porcine reproductive and respiratory syndrome virus (Guo et al., 2013). An increased endogenous miR-206 expression is observed in pigs infected with influenza A H1N2 subtype at a later stage of the infection (Kerstin et al., 2013). However, miR-206 regulation of influenza virus replication has not been demonstrated yet.

Type I interferons (IFNs) play an important role in innate immunity against viral infections (Ehrhardt etal., 2010; Garcia-Sastre, 2011). Cellular host factors that induce IFNs and thus activate anti-viral state in cells could determine the fate of viral infections. One class of such host factors are miRNAs that act as critical regulators of IFNs and IFN-stimulated genes during viral infection (Forster, Tate, & Hertzog, 2015; Sedger, 2013). In addition to regulating genes, some miRNAs such as miR-136 has been shown to trigger innate immunity by acting as a ligand for RIG-I (L. Zhao et al., 2015).

The objectives of this study are to investigate the roles of TNKS2 in influenza virus infection, identify the miRNAs that target TNKS2, and understand the mechanisms involved. We found that TNKS2 expression was elevated during IAV infection and reduction in TNKS2 levels by RNA interference inhibited IAV replication. miR-206 was identified as one of the miRNAs that targets TNKS2. miR-206 suppressed IAV infection by activating an anti-viral state.

2 | RESULTS

2.1 | Influenza virus induces TNKS2 expression

Human cytomegalovirus was reported to alter TNKS expression (Roy et al., 2016). We first examined the effects of influenza virus infection on TNKS2 expression. Lung epithelial A549 cells were infected with an MOI of 0.01 of A/PR/8/34 for various times and TNKS2 expression was determined. Viral NP protein expression was increased by IAV infection, confirming efficient infection of IAV (Figure 1a,b). A gradual increase in the TNKS2 protein level was observed as a function of infection time (Figure 1a,b). TNKS2 mRNA levels

exhibited infection time-dependent and dose-dependent increases (Figure 1c,d). Similar results were also observed in HEK293 cells (Figure S1a–c). Furthermore, TNKS2 mRNA expression was elevated in A549 cells infected with different strains of IAV including H1N1 A/PR/8/34, A/WSN/1933, A/Oklahoma/3052/2009, and H3N2 A/Okla-homa/309/2006 (Figure 1e). TNKS2 protein levels were also increased by different strains of IAV (percentage of control: A/PR/8/34, 196 ± 126%; A/WSN/1933, 137 ± 118%; A/Oklahoma/3052/2009, 159 ± 115%; and H3N2, 201 ± 128%) (Figure S1d,e). These results suggest that TNKS2 induction by IAV is not strain-dependent. An increase in TNKS2 protein expression was also observed in the lungs of the mice infected with a sub-lethal dose of A/PR/8/34 at 3 and 7 dpi (Figure 1f,g). Collectively, these results suggest that IAV infection increases TNKS2 protein expression in vitro and in vivo.

2.2 | Knockdown of TNKS2 reduces viral replication

To assess the role of TNKS2 in IAV replication, we knocked down TNKS2 expression and evaluated IAV replication. HEK 293 cells were transfected with plasmids expressing three different TNKS2 shRNAs or its control (shCon), followed by infection with A/PR/8/34. TNKS2 and viral protein levels in cells and virus titers in media were determined by western blot and $TCID_{50}$ assay, respectively. We observed that shTNKS2–1 and shTNKS2–3, but not shTNKS2–2 reduced TNKS2 levels, viral NP protein expression, and virus production (Figure 2a–c). shTNKS2–1 showed a similar effect on viral protein levels and viral titers in A549 cells (Figure S2a–c). Taken together, these results show that the knockdown of TNKS2 expression inhibits IAV replication.

2.3 | Identification of miRNAs that target TNKS2

As shRNA targeting TNKS2 can inhibit IAV infection, we wonder whether we could use a miRNA as a tool to suppress endogenous TNKS2 and thus IAV infection. To identify the miRNAs that target TNKS2, we used TargetScan software (version 6.1) (http://www.targetscan.org/) to predict the miRNA binding sites on the 3'-UTR of human TNKS2. We found that TNKS2 3'-UTR has the conserved binding sites for 30 miRNAs. All of the miRNAs have one binding site except miR-206 that has three binding sites. miR-17/20b/93/106ab/518/519, miR-141/200a, miR-105/520be/302abce/372/373 and miR-1,297/26ab each share the same binding site. We then used 3'-UTR luciferase reporter assay to experimentally validate the prediction by overexpressing each miRNA. We found that 5 miRNAs significantly inhibited the reporter activities in A459 cells (Figure 3a). Among them, only miR-206 and miR-106b caused approximately 50% reduction of the reporter activities. Thus, we selected these two miRNAs for further evaluation of anti-IAV activities.

2.4 | miR-206 suppresses influenza a virus replication

To evaluate the effects of miR-206 and miR-106b on influenza virus infection, we overexpressed these miRNAs and examined viral protein and mRNA levels as well as viral titers. HEK293 cells were transfected with a miRNA expression plasmid, which contains EGFP marker. GFP images revealed a high transfection efficiency for miR-206 and miR-106b expression plasmids (Figure 3b). Real-time PCR analysis indicated that miR-206 and miR-106b levels were higher in the miRNA-transfected cells than the control, miR-Con

(Figure 3c). It is noted that the endogenous miR-206 level in HEK293 cells was significantly lower than that of miR-106b. Overexpression of miR-206, but not miR-106b reduced viral NP and NS1 protein expression (Figure 3d,e). miR-206 also inhibited viral NP, NS1 and PB1 mRNA expression (Figure 3f) and virus titre in the medium as determined by $TCID_{50}$ assay (Figure 3g). Furthermore, miR-206 suppressed the replication of different strains of influenza A virus including H1N1 A/PR/8/34, A/WSN/33, A/Oklahoma/3052/09 (2009 pandemic strain) and H3N2 A/OK/309/06 as determined by an IAV reporter assay (Figure 3h). miR-206 also reduced the protein levels of viral NS1, the mRNA levels of viral NS1, NP and PB1 and virus production in A549 cells (Figure S3a–f). Collectively, these results suggest that miR-206 inhibits H1N1 and H3N2 influenza virus infection in HEK293 and A549 cells.

2.5 | miR-206 reduces endogenous TNKS2 expression

There are three conserved binding sites of miR-206 on TNKS2 3'-UTR as predicted by TargetScan (Figure 4a). 3'-UTR reporter assay confirmed the binding of miR-206 to 3'-UTR of TNKS2 (Figure 3a). We further determined whether miR-206 can reduce the endogenous TNKS2 expression. Overexpression of miR-206 in A549 cells decreased the TNKS2 protein expression in A549 cells with and without IAV infection (Figure 4b,c). Additionally, miR-206 overexpression suppressed the mRNA expression of TNKS2 (Figure 4d). A similar reduction in TNKS2 protein and mRNA levels was also observed in miR-206-overexpressed HEK293 cells (Figure S4a–c). These results suggest that miR-206 reduces TNKS2 expression via mRNA degradation.

If TNKS2 is a target of miR-206, we expect that the miR-206 level would be decreased by IAV because IAV increased TNKS2 expression (Figure 1). Indeed, endogenous miR-206 expression was gradually decreased by A/PR/8/34 in a time-and virus dose-dependent manner in A549 cells (Figure 4e,f) and HEK293 cells (Figure S4d,e). IAV also decreased the expression of miR-206 in the primary cells, HBTEC and the lungs of C57BL/6 mice (Figure 5g,h).

We next examined whether a change in TNKS2 level influences miR-206 expression. We overexpressed TNKS2 in HEK293 cells and measured the miR-206 expression. TNKS2 overexpression had no effects on miR-206 expression (Figure S4f,g).

2.6 | miR-206 induces an anti-viral state

Cells synthesise IFNs to prime cells to an antiviral state in response to a viral infection. Thus, we investigated whether miR-206 induces type I IFN response. miR-206-overexpressed HEK293 cells and A549 cells were infected with A/PR/8/34 at a MOI of 0.01. miR-206 increased mRNA expression of type I IFNs, IFN-β1 and IFN-α1 at 24 hpi in HEK293 cells (Figure 5a,b) and at 48 hpi in A549 cells (Figure S5a,b). miR-206 did not significantly change the type I IFN mRNA levels in uninfected HEK293 cells (Figure 5a,b) and A549 cells (Figure S5a,b).

IFN induction requires the JNK-dependent activation of IRF3 and c-Jun (Yoshizawa, Hammaker, Sweeney, Boyle, & Firestein, 2008). Thus we examined the effects of miR-206 on the activation of JNK/c-Jun signalling. miR-206 increased the phosphorylation of JNK

and c-Jun (Figure 5c–e). miR-206 also increased the JNK luciferase reporter activity (Figure 5f).

Type I IFNs activate JAK/Stat signalling cascade, which leads to an increase in the expression of IFN-stimulated genes (ISGs). The phosphorylation of Stat1 is the key to activate this signalling pathway. Therefore, we examined the effects of miR-206 on the phosphorylation of Stat1 during IAV infection. miR-206 enhanced the phosphorylation of Stat1 in HEK293 (Figure 5g,h) and A549 cells (Figure S5c,d). The phosphorylation of Stat1 leads to the formation of Stat1/2 dimers, which translocate into nuclei and bind ISRE to activate ISGs. miR-206 increased the transcriptional activity of ISRE as determined by an ISRE luciferase reporter assay (Figure 5i). Furthermore, miR-206 also increased the mRNA expression of ISGs, OAS1, and MX1 in HEK293 (Figure 5j) and A549 cells (Figure S5e). Collectively, these data suggest that miR-206 activates type I IFN response and primes the cells to an anti-viral state.

2.7 | miRNA-206 overexpression in the lungs reduces viral load and increases survival from IAV infection

Virus-based vector systems such as retroviruses, adenoviruses or adeno-associated viruses have been used to deliver miRNAs into the lungs in vivo (Yang, 2015). We used an adenovirus expressing miR-206 (Ad-miR-206) or its control (Ad-miR-Con) to investigate its anti-viral activity in vivo and underlying mechanisms. Adenovirus was delivered into the lungs of mice intratracheally. The mice were infected with a sub-lethal dose of A/PR/8/34 at day 0. Lungs tissues were collected at 3 and 7 dpi. miR-206 expression in the lungs of Ad-miR-206-treated mice was increased at 3 and 7 dpi compared to these of the Ad-miR-Con group (Figure 6a).

Ad-miR-206 reduced virus production by 17-fold in the lung tissue at 7 dpi (Figure 6b). Ad-miR-206 also inhibited viral NP and NS1 protein expression by 52 ± 12% and 75 ± 18%, respectively at 7 dpi (Figure 6c–e). To further confirm the miR-206 effect on viral infection in mouse lungs, viral NP protein in the lung tissue sections from A/PR8/34-infected mice at 7 dpi was stained by immunofluorescence using anti-NP antibodies. Ad-miR-206 reduced the percentage of infected cells (NP-positive cells) in the alveolar region (Figure 6f,g). Furthermore, Ad-miR-206 reduced mRNA expression of viral PB1 and NS1 at 3 and 7 dpi (Figure 6h). It is noted that viral protein levels in the lung tissues of Ad-Con groups were higher at 7 dpi than these at 3 dpi (Figure 6c–e). However, viral mRNA levels were higher at 3 dpi than these at 7 dpi (Figure 6h).

To determine whether miR-206 protects mice from influenza virus infection, we performed a survival study. Ad-miR-206 significantly increased the survival of mice compared to Ad-miR-Con (Figure 6i). Moreover, mice expressing miR-206 in the lungs had a lower clinical score (Figure 6j). Collectively, these results suggest that miR-206 protects mice against influenza virus infection.

To determine the mechanisms of miR-206 action in vivo, we examined the expression of miR-206 target proteins and the associated components in the pathways involved. TNKS2 protein expression was suppressed by Ad-miR-206 at 3 dpi, but not at 7 dpi (Figure 7a,b).

The mRNA expression of TNKS2 was also reduced at 3 dpi by Ad-miR-206 (Figure 7c). Furthermore, the phosphorylation of JNK, c-Jun, and Stat1 in the lungs was significantly increased by Ad-miR-206 at 7 dpi (Figure 7a,d–f). The protein levels of total Stat1, but not total JNK and c-Jun protein were increased from 3 dpi to 7 dpi in both Ad-miR-Con and Ad-miR-206 groups, suggesting that Stat1 is also regulated at the protein level during IAV infection, in addition to phosphorylation. Ad-miR-206 enhanced the mRNA expression of type I IFNs, IFN-α1 (49 ± 11%) and IFN-β1 (35 ± 20%) and type III IFN, IFN-λ2 (19 ± 7%) at 7 dpi, but not 3 dpi (Figure 7g). It is noted that IFN-α1 mRNA expression was reduced at a later stage of the infection compared to IFN-β1 and IFN-λ2. Ad-miR-206 also augmented the expression of ISG, OAS1 (Figure 7h). Taken together, these data suggest that miR-206 inhibits IAV infection in mice by activating anti-viral state.

3 | DISCUSSION

Error-prone replication and genetic reassortment of the influenza virus result in its resistance to the current anti-viral drugs, which target viral proteins. Influenza virus requires host factors to complete its life cycle (Konig et al., 2010; Tripathi, Batra, & Lal, 2015). Thus identifying host factors that are involved in influenza virus replication may pave the way to develop novel therapeutics. Cellular miRNAs play important roles in many biological processes including viral infection. In this study, we found that (a) IAV induced endogenous TNKS2 expression in cell culture and mouse lungs, (b) TNKS2 knockdown inhibited IAV replication, (c) miR-206 inhibited IAV infection in vitro and in vivo by inducing an anti-viral state, and (d) Importantly, overexpression of miR-206 in the lungs of mice increased survival against IAV infection.

Influenza viruses are obligate intracellular parasites that either coopt or subvert various cellular processes in order to hijack the host machinery and evade the host immune responses. Influenza viruses affect many cellular pathways such as mitogen-activated protein kinase (MAPK) pathway, TLR/RIG-I signalling, NF-κB signalling, PI3K/Akt pathway, JAK/Stat and PKC/PKR signalling (S. Ludwig, 2009; Gaur, Munjhal, & Lal, 2011). Our study demonstrates that mRNA and protein expression of endogenous TNKS2 were induced during IAV replication. This is consistent with TNKS1/2 induction by human cytomegalovirus (HCMV) (Roy et al., 2016). However, herpes simplex virus (HSV) infection decreases TNKS1, but not TNKS2 protein expression at 24 hpi (Z. Li, Yamauchi, et al., 2012). The protein-protein interaction network analysis of human TNKS1/2 identifies over 100 interacting proteins, potentially leading to changes in numerous biological functions such as transcription, WNT signalling and NF-κB pathway (X. Li, Han, 2017). Activating WNT and NF-κB pathways have been shown to promote IAV replication (S. Ludwig & Planz, 2008) (More et al., 2018). TNKS1/2 also reduces the protein level of Axin, a negative of WNT signalling (S. M. Huang, Mishina, et al., 2009). Therefore, TNKS2 upregulation during IAV infection may lead to the alteration in cellular signalling to aid virus replication.

Our present studies showed that knockdown of TNKS2 reduced influenza viral protein levels and titers in both HEK293 and A549 cells, suggesting that TNKS2 is a novel host factor that positively regulates IAV replication. Positive and negative effects of TNKS on the infection

of herpesvirus, a DNA virus have been reported. The knockdown of TNKS1 or TNKS2 or inhibition of TNKS activity with XAV939 decreases the replication of HSV (Z. Li, Yamauchi, et al., 2012). During HSV infection, the early viral protein ICP0 recruits TNKS1, but not TNKS2 to nuclei to facilitate its replication, suggesting different mechanisms for TNKS1 and TNKS2 to promote HSV replication. On the other hand, TNKS2 negatively regulates Epstein–Barr virus replication by interacting with Epstein–Barr virus nuclear antigen 1, requiring TNKS2 PARP activity (Deng et al., 2005). TNKS inhibition also facilitates the efficient replication of HCMV (Roy et al., 2016). Collectively, our observation and previous findings suggest that the effects of TNKS on virus replication are virus-dependent.

In the current study, we found that endogenous miR-206 levels were significantly decreased in IAV H1N1-infected cells in culture and the lungs of mice. In contrast, pigs challenged with IAV H1N2 showed an increased expression of miR-206 in the lungs (Kerstin et al., 2013). Chicken infected with the avian influenza virus also exhibited an upregulation of miR-206 in the lung although a downregulation in the trachea (Wang et al., 2009). These results indicate that miR-206 regulation during IAV infection is species- and strain-specific although our current studies have shown that overexpression of miR-206 inhibits IAV H1N1 and H3N2 infection in both HEK293 and A549 cells. Several studies suggest that miR-206 could be used as a biomarker for diseases with a viral origin. A rise in serum miR-206 has been observed in patients with hepatitis B virus-related hepatocellular carcinoma (Tan et al., 2015). The upregulation of miR-206 in Olfactory bulb and trigeminal ganglia is associated with Aujeszky’s disease in pigs (Timoneda et al., 2014).

In the current studies, we identified miR-206 as a miRNA that targets TNKS2. We also demonstrated that miR-206 inhibited IAV replication in cells using various IAV strains including clinical isolates of H1N1 pdm/Ok/2009 and H3N2 A/OK/309/06 and in mice using A/PR/8/34. miR-206 was also reported to limit the replication of other viruses including respiratory syndrome virus and porcine reproductive and respiratory syndrome virus (Guo et al., 2013). Furthermore, a decrease in the miR-206 level appears to play a critical role in the pathological outcome of simian immunodeficiency virus (SIV)-infected macaques where miR-206 inhibitor decreases myotube differentiation in skeletal muscle and results in impaired muscle function (Simon et al., 2017).

With regards to the mechanisms of miR-206-mediated anti-IAV activities, there are two possibilities: targeting viral proteins themselves or targeting host factors. miRNAs such as miR-323, miR-491, miR-654, and miR-let-7c can directly bind 3’-UTR of influenza viral genes to attenuate virus replication (He, Feng, Chen, Wang, & Wang, 2009; Y.-J. Ma, Yang, et al., 2012; Song et al., 2010). However, miR-206 does not possess the binding sites in IAV 3’-UTRs. Thus the direct binding with viral 3’-UTR is not likely a mechanism for miR-206 action on IAV replication.

Our data support that miR-206 activates IFN responses during IAV infection by the following in vitro and in vivo observations: (a) miR-206 induced mRNA expression of type I IFNs during IAV infection, (b) miR-206 increased the phosphorylation of Stat1, (c) miR-206 enhanced transcriptional activity of Stat1 as demonstrated by an ISRE reporter assay, and (d)

miR-206 induced the expression of ISGs. The activation of MAPK is essential for downstream type I IFN signalling (Goh, Haque, & Williams, 1999; L. J. Zhao, Hua, He, Ren, & Qi, 2011). Our results showed that miR-206 increased the phosphorylation of JNK and c-Jun. Thus the activation of JNK/c-Jun signalling by miR-206 is a possible mechanism for miR-206-mediated type I IFN production. miR-136 and miR-302c have been shown to enhance IFN responses during IAV infection by targeting the RIG-1 pathway (L. Zhao, Zhu, et al., 2015) and NF-kappaB (Gui et al., 2015), respectively.

We observed that Stat 1 protein level was increased in mouse lungs during IAV infection from 3 dpi to 7 dpi, which is consistent with two previous studies in mouse embryo fibroblasts and mouse lung tissue (García-Sastre et al., 1998) (S. Zhang, Huo, et al., 2019). Furthermore, Stat 1 deletion in mice showed 100-fold more susceptible to IAV infection (García-Sastre et al., 1998). Thus, the activation of Stat1 signalling is likely due to increases in both protein levels and phosphorylation status of Stat 1 at the later-stage of IAV infection in mouse models.

Type III IFN responses are mediated through IFN-λ. Like type I IFN, type III IFN also utilises the JAK/STAT pathway to activate ISG (Davidson et al., 2016). Typical barrier tissues such as mucosal epithelial cells are more responsive to IFN-λ (Wack, Terczynska-Dyla, & Hartmann, 2015). Furthermore, airway epithelial cells express IFN-λ as the major IFN induced by respiratory viruses (Egli, Santer, O'Shea, Tyrrell, & Houghton, 2014). We observed IFN-λ2 was significantly induced by IAV infection in the lungs of mice at 3 dpi and sustain through 7 dpi. Importantly, we observed that similar to type I IFNs, miR-206 induced IFN-λ2 expression at the late stage of IVA infection where we observed a reduced viral load in the mouse lungs.

Some miRNAs have reached the stage of clinic trials, for example, miR-122 for treating Hepatitis C virus and miR-155 for treating haematological malignancies (Christopher et al., 2016). However, clinical applications of miRNAs face many challenges such as limitations in delivery vectors of miRNA modulators, testing of delivery vector capacities, and degradation of naked particles in vivo (Chen, Zhao, Tan, Zhang, & Fu, 2015). Although several studies examined miRNA regulation of IAV infection, few investigated the potential of miRNAs as anti-viral agents in vivo. Our current studies showed that the adenovirus vector system successfully delivered miR-206 into mouse lungs, resulting in a reduced virus load. Our findings may expand our knowledge of potential targets for developing anti-influenza therapeutics.

In summary, we identified miR-206 as a miRNA targeting TNKS2 and showed that miR-206 inhibited IAV infection in vitro and in vivo through the activation of anti-viral innate immunity via type I IFNs.

4 | EXPERIMENTAL PROCEDURES

4.1 | Cell culture

Human embryonic kidney (HEK293 and HEK293T), human lung epithelial (A549) and Madin-Darby canine kidney epithelial (MDCK) cells were purchased from the American

Type Culture Collection (ATCC, Manassas, VA). Primary human bronchial tracheal epithelial cells (HBTEC) were obtained from Lifeline Cell Technology (Frederick, MD). HEK and MDCK cells were maintained in DMEM media with 10% fetal bovine serum (FBS) and 1% penicillin and streptomycin (PS), while A549 cells were maintained in F12K medium with 10% FBS and 1% PS. HBTEC cells were maintained in BronchiaLife™ Complete Medium (Lifeline Cell Technology, Cat # LL-0023). The cells with a passage number of less than 22 and 8 were used for A549 and HEK293 cells, and HBTEC cells, respectively.

4.2 | Viruses

The H1N1 strain of influenza virus A/PuertoRico/8/34 (A/PR/8/34) were purchased from ATCC. H1N1 A/WSN/1933 (A/WSN/33), H1N1 A/Oklahoma/3052/2009 (pdm/Ok/09) and H3N2 A/Oklahoma/309/2006 (A/OK/309/06) were a gift from Dr. Gillian Air (University of Oklahoma Health Sciences Center). The viruses were propagated in the allantoic cavities of 10-day-old specific-pathogen-free embryonated chicken eggs (Charles River Laboratories, MA, USA) at 35°C. The allantoic fluid harvested from the infected eggs was centrifuged at 2,000g for 10 min and stored at −80° C.

4.3 | Vector construction

shRNA vectors: A short hairpin RNA (shRNA) of human TNKS2 (Table S1) was cloned into a lentiviral pmiRzip vector (System Biosciences, Mountain View, CA) as previously described (C. Huang, Xiao, et al., 2017). A vector containing a scrambled shRNA (shCon) was used as the control.

miRNA and TNKS2 expression vectors: Mature miRNAs and their flanking sequences (~ 200 bp at each end) were PCR-amplified by using specific primers (Table S1) and human genomic DNA. PCR products were cloned into a modified pENTR vector, which can be switched to an adenoviral vector or a modified pLVX-Puro lentiviral vector (Clontech, Mountain View, CA) between EGFP and VS40 poly A terminal sequence through Xho I and EcoR I sites as previously described (C. Huang, Xiao, et al., 2017). Both vectors use CMV promoter to drive EGFP-miRNA expression. A similar size of genomic DNA that did not contain any miRNAs or stem-loop structures was used as the control vector (miR-Con). TNKS2 overexpression vector (pFlag-CMV2-TNKS2) and its control vector (pFlag-CMV2-Control, were obtained from Addgene (Watertown, MA) and Sigma-Aldrich (St. Louis, MO), respectively.

TNKS2 3'-UTR reporter vector: The 3'-UTR of human TNKS2 were amplified by PCR using human genomic DNA and a primer pair listed in Table S1. PCR products were cloned into a pmirGLO Dual-Luciferase (Firefly and *Renilla*) miRNA target expression vector (Promega, Madison, WI) through Sal I and NheI restriction sites at the downstream of a firefly luciferase reporter gene.

4.4 | Lentivirus and adenovirus production

Lentiviral shRNA or miRNA and control vectors were co-transfected along with psPAX2 (packaging plasmid) and pMD2G (envelop plasmid) into HEK293T cells by using 6 μg

polyethylenimine (PEI) (Sigma) per μg plasmid. The lentiviruses produced were collected and stored at −80°C. The titre was determined in HEK293T cells as previously described (C. Huang, Xiao, et al., 2017).

For producing adenovirus, miR-206 or miR-Con in the pENTR vector was switched to pAd/PL-DEST™ adenoviral vector (Invitrogen, Carlsbad, CA) through LR recombination. After digestion and linearisation by PacI, the adenovirus vector was transfected into HEK293A cells. Seventy-two hours post-infection, cells and media containing adenovirus were harvested and further amplified by reinfecting HEK293A cells. The crude viral lysate was obtained after several freeze/thaw cycles and centrifugation. Subsequently, adenovirus was purified and concentrated by using Adeno-X Maxi purification kit (Clontech, Mountain View, CA). Virus titre was determined by infecting HEK 293A cells with a series of dilutions of the viral stock and counting GFP-positive cells.

4.5 | Influenza virus infection

HEK293 cells were cultured in a 12-well plate (5×10^5 cells/well) for 24 hr and transfected with pENTR miRNA expression or control plasmid for 24 hr by using Lipofectamine 3,000 (Invitrogen). A549 cells were seeded in a 12-well plate (2×10^5 cells/well) for 24 hr and transduced with a lentivirus expressing shRNA, miRNA or respective control at a multiplicity of infection (MOI) of 100 in the presence of polybrene (Sigma, 10 μg/ml) for 48 hr. Cells were infected with A/PR/8/34 at various MOIs in a serum-free medium for 1 hr. The inoculation media were then replaced with serum-free media containing 0.3% bovine serum albumin (BSA), and 0.5 μg/ml trypsin-treated with L-(tosylamide-2-phenyl) ethyl chloromethyl ketone (TPCK, Worthington Biochemical Corporation, Lakewood, NJ). At different incubation times, cells and media were collected for determining mRNA and protein expression and virus titre, respectively.

4.6 | Real-time PCR

Total RNAs were isolated using TRI Reagent (Molecular Research Center, Cincinnati, OH). One μg of RNA was treated with RNase-Free DNase I (ThermoFisher Scientific, Waltham, MA) at 37°C for 30 min and reverse-transcribed into cDNA by using oligo (dT), random primers and Moloney murine leukaemia virus (M-MLV) reverse transcriptase (Promega).

Real-time PCR was carried out in a 20-μl reaction containing gene-specific primers (Table S2) and SYBR green PCR master mix (Eurogentec, Fremont, CA). PCR was performed on ABI 7500 realtime PCR System (Applied Biosystems, Foster City, CA). Cycling conditions were as follows: 95°C for 1 min, followed by 40 cycles of 95°C for 15 s and 60°C for 1 min. β-actin was used as a housekeeping gene. The expression level of a target mRNA relative to the housekeeping gene was calculated using the comparative Ct method ($2^{-\Delta Ct}$).

For miRNA quantitation, total RNA was first subjected to Poly-A tailing. Briefly, a 10-μl reaction containing 1 μg of total RNA, 1 μl of 10x reaction buffer, 1 μl of 10 mM ATP and 5 units of *E. coli* poly(A) polymerase (New England Bio Labs, Ipswich, MA) was incubated at 37°C for 20 min, followed by enzyme inactivation at 65°C for 20 min. Subsequently, the product was reverse-transcribed into cDNA using Poly-T-Adaptor (New England Bio Labs), dNTP and M-MLV reverse transcriptase. PCR was performed using a specific forward

primer for a mature miRNA and general reverse primer (Table S2) and SYBR green PCR master mix as previously described (L. Zhang, Huang, et al., 2015). U6 small nuclear RNA (snRNA) was used as an internal control.

4.7 | Western blotting

Cells or tissues were lysed in protein lysis buffer with 1x Halt™ Protease and Phosphatase Inhibitor Cocktail (ThermoFisher Scientific) for 10 min at room temperature and centrifuged at 3,000 × *g* for 5 min. Protein concentrations in the supernatant were measured using the Bio-Rad protein assay kit (Bio-Rad, Hercules, CA). Ten microgram of total proteins were separated on 10% sodium dodecyl sulfate-polyacrylamide gel electrophoresis (SDS-PAGE) and transferred to nitrocellulose membrane. Membranes were blocked with 5% skimmed milk in ×1 Tris-buffered saline with 0.1% Tween-20 (TTBS) for 1 hr and incubated overnight with primary antibodies: mouse anti-NS1 (1:1,000, sc-130,568, Santa Cruz, Dallas, TX), mouse anti-NP (1:50, HB-65, ATCC), rabbit anti-TNKS2 (1:1,000, ab155545, Abcam, Cambridge, MA), rabbit anti-p-JNK (1:1,000, CS-4668S, Cell Signalling, Danvers, MA), rabbit anti-JNK (1:1,000, CS-9252S, Cell Signalling), rabbit anti-p-c-Jun (1:1,000, CS-2361S, Cell Signalling), rabbit anti-c-Jun (1:1,000, SC-1694, Santa Cruz), rabbit anti-p-Stat1 (1:1,000, CS-9167S, Cell Signalling), rabbit anti-Stat1 (1:1,000, CS-14994S, Cell Signalling), and mouse β-actin (1:1,000, MA5–11869, ThermoFisher Scientific,) After proper washing with TTBS, membranes were then incubated with horseradish peroxidase-conjugated goat anti-rabbit or goat anti-mouse (1:1,000) secondary antibodies for 1 hr. Membranes were washed again, and target proteins were visualised using the SuperSignal™ West Pico PLUS chemiluminescent substrate (ThermoFisher Scientific).

4.8 | $TCID_{50}$ assay

Virus titre was determined by a Tissue Culture Infective Dose ($TCID_{50}$) assay. Briefly, MDCK cells (1.5×10^4/well) seeded in 96 well plates were washed with serum-free media and infected in four replicates with a series of 10-fold dilutions of virus stocks in serum-free medium containing 1 μg/ml TPCK-trypsin. Cells were analysed for the cytopathic effect after 72 hr post-infection (hpi). $TCID_{50}$ was calculated as previously described (Reed & Muench, 1938).

4.9 | Dual-luciferase assay

3'-UTR reporter assay: A549 cells were seeded in a 96 well plate (1×10^6 cells/plate) and cultured for 24 hr. Subsequently, cells were co-transfected with 5 ng of pmirGLO-firefly-TNKS2-3'-UTR vector and 100 ng pENTR miRNA expression plasmid or its control (miR-Con) by using Lipofectamine 3,000 (Invitrogen). Cells were incubated 24 hr. Forty microliter of passive lysis buffer was added to each well and shaken for 5 min. After brief centrifugation (12,000 g for 5 min at 4°C), 10 μl of the supernatant was taken for the dual-luciferase reporter assay using the Dual-Luciferase Assay System Kit (Promega, Madison, WI) and the FLUOstar OPTIMA microplate fluorometer (BMG LABTECH, Offenburg, Germany). Firefly luciferase activities were normalised to *Renilla* luciferase activities.

Influenza virus reporter assay: HEK293 cells were co-transfected with pENTR miRNA or miR-Con plasmid (100 ng), IAV luciferase reporter plasmid, pHH21-NP-3'-UTR-Luc-

NP-5'-UTR (20 ng) and pRL-TK *Renilla* luciferase plasmid (20 ng) (More et al., 2018). Twenty-four hours post-transfection, the cells were infected with A/PR/8/34, A/WSN/33, pdm/Ok/09, A/OK/309/06 at an indicated MOI. Forty-eight hours post-infection (hpi), cells were lysed and dual luciferase activities were measured as described above.

Pathway reporter assay: HEK293 cells were transfected with 50 ng of JNK luciferase reporter plasmid or interferon-stimulated response elements (ISRE) luciferase reporter plasmid (QIAGEN, Germantown, MD, USA), 10 ng of pRL-TK *Renilla* luciferase plasmid and 100 ng pENTR miRNA expression or miR-Con plasmid for 24 hr. Subsequently, cells were infected with A/PR/8/34 virus at a MOI of 0.01. Samples were collected at 48 hpi and dual luciferase activities were measured as described above.

4.10 | Animal studies

Female C57BL/6J mice (8–9 weeks old) were obtained from Jackson Laboratory (Bar Harbour, ME). Experimental protocols were reviewed and approved by the Institutional Animal Care and Use Committee (IACUC) of Oklahoma State University. Two days before influenza virus infection (−2 dpi), an adenovirus expressing miR-206 (Ad-miR-206) or miR-Con (Ad-miR-Con) (1×10^9 infectious unit in 50 μl) was delivered intratracheally into the lungs of mice after intraperitoneal injections of ketamine and xylazine. At 0 dpi, mice were infected intranasally with A/PR/8/34 (250 plagues forming unit in 50 μl). Mice were euthanised at 0, 3 or 7 dpi. The left lungs were fixed in 10% neutral buffered formalin (ThermoFisher Scientific) and right lungs were snap-frozen in liquid nitrogen. The right lungs were powdered under liquid nitrogen by using mortar and pestle, aliquoted into three fractions and stored at −80°C for further use. One aliquot of lung tissue was dissolved in DMEM medium, subjected to three freeze/thaw cycles and used for virus titre determination by $TCID_{50}$ assay. Remaining two aliquots were lysed in tissue lysis buffer (ThermoFisher Scientific) for western blot analysis or in TRI Reagents for real-time PCR analysis.

For survival studies, mice were treated with the same dose of Ad-miR-206 or Ad-miR-Con at −2 dpi as described above and challenged with 1x mouse lethal dose 50 (MLD50) of A/PR/8/34. Mice were monitored daily for bodyweight loss and clinical signs. Clinical scores were graded according to the modified procedure of (Tate, Brooks, & Reading, 2008): 0 = normal, 1 = slightly ruffled fur (fur standing up or in irregular or disturbed lining of the fur; typically in part of the body), 2 = ruffled fur (fur standing up or in irregular or disturbed lining of the fur in whole body) and hunched back (a back deformed by a sharp forward angle, forming a hump), 3 = ruffled fur, hunched back, reduce activity (less social interactions, not actively moving around in the cage) and rapid breathing (increased respiratory rate), 4 = ruffled fur, hunched back, reduce activity and laboured breathing (an abnormal respiration characterised by evidence of increased effort to breathe including the use of accessory muscles of respiration, stridor, grunting or nasal flaring), 5 = lost more than 30% of their body weights, or abdominal breathing (an abnormal respiration characterised by evidence of increased effort to breathe, including the use of accessory muscles of respiration, stridor, grunting, or nasal flaring as well as diaphragm and the abdominal muscles), dehydration (skin tenting; the skin maintains a triangular or tent-like appearance when gently pinched) and minimal mobility (not moving about, unresponsive or minimal

responsive to provocation) or moribund. Mice that reached a clinical score of 5 were euthanised.

4.11 | Immunofluorescence

Four micrometre paraffin-embedded lung tissue sections were deparaffinised by incubation in xylene for 10 min and sequential incubation (10 min each) in ethanol gradient (100, 95, 50, and 0%). The sections were boiled in citrate buffer (10 mM, pH 6) for 10 min for antigen retrieval. Subsequently, sections were washed 1% Tween-20 in PBS (PBST) and blocked with mouse Ig blocking reagent (Vector Lab, Cat#MKB-2213) for 1.5 hr at 37°C. The section was then incubated with primary antibodies, mouse anti-NP (1:20; ATCC) in PBST containing 1% BSA for 1 hr at 37°C. After incubation, sections were washed with PBST and incubated with Alexa fluor 546-conjugated goat anti-mouse secondary antibodies (1:200, Invitrogen) at 37°C for 1 hr, followed by incubation with 2 μg/ml of Hoechst 33342 dye for 10 min. Sections were washed with PBST and mounted with Pro-Long™ gold anti-fade reagents (ThermoFisher Scientific). Images were captured by Photometrics CoolSnap CCD camera (Roper Scientific) and processed by Metavue software (Universal Imaging Co.). The NP staining of alveolar regions was quantified by a blinded investigator. For each section, five images were taken randomly from alveolar regions with a × 20 objective. Total cells and NP-positive cells were counted to determine the percentage of NP-positive cells.

4.12 | Data analysis

Data from at least three independent experiments were analysed. Six or more animals were used for in vivo experiments. Statistical tests were performed using Graph Pad Prism version 6.0. Studen's *t* test was used for two groups and one-way or two-way analysis of variance (ANOVA), followed by post hoc dunnet's or Sidak's pairwise comparison was used for multiple groups. A p value of $<.05$ was considered significant.

Supplementary Material

Refer to Web version on PubMed Central for supplementary material.

ACKNOWLEDGMENTS

We thank Dr. Gillian Air (University of Oklahoma Health Sciences Center) for providing WSN, pdm09, and H3N2 A/Oklahoma/309/2006. This work was supported by the National Institutes of Health grants AI121591, HL135152, and GM103648, the Oklahoma Center for the Advancement of Science and Technology: HR-20-050, the Oklahoma Center for Adult Stem Cell Research-A Program of Tobacco Settlement Endowment Trust (TSET) and the Lundberg-Kienlen Endowment fund (to LL).

Funding information

the Lundberg-Kienlen Endowment fund the National Institutes of Health, Grant/Award Number: GM103648, AI121591, HL135152; the Oklahoma Center for the Advancement of Science and Technology, HR-20-050 the Oklahoma Center for Adult Stem Cell Research-A Program of Tobacco Settlement Endowment Trust (TSET)

REFERENCES

Bartel DP (2004). MicroRNAs: Genomics, biogenesis, mechanism, and function. Cell, 116(2), 281–297 Retrieved from http://ac.els-cdn.com/S0092867404000455/1-s2.0-S0092867404000455-main.pdf?

_tid=f54fe340-6805-11e6-9fc9-00000aacb35f&acdnat=1471828728_18b2f35a991fce001c47b0b0a7e71d92 [PubMed: 14744438]

Bouvier NM, & Palese P (2008). The biology of influenza viruses. Vaccine, 26(Suppl 4), D49–D53 Retrieved from http://www.ncbi.nlm.nih.gov/pmc/articles/PMC3074182/ [PubMed: 19230160]

Center of Disease Control. (2020, 4 17). Disease Burden of Influenza. Retrieved from https://www.cdc.gov/flu/about/burden/index.html

Chen Y, Zhao H, Tan Z, Zhang C, & Fu X (2015). Bottleneck limitations for microRNA-based therapeutics from bench to the bedside. Pharmazie, 70(3), 147–154. [PubMed: 25980175]

Christopher AF, Kaur RP, Kaur G, Kaur A, Gupta V, & Bansal P (2016). MicroRNA therapeutics: Discovering novel targets and developing specific therapy. Perspectives in Clinical Research, 7(2), 68–74. 10.4103/2229-3485.179431 [PubMed: 27141472]

Davidson S, McCabe TM, Crotta S, Gad HH, Hessel EM, Beinke S, … Wack A (2016). IFNlambda is a potent anti-influenza therapeutic without the inflammatory side effects of IFNalpha treatment. EMBO Molecular Medicine, 8(9), 1099–1112. 10.15252/emmm.201606413 [PubMed: 27520969]

Deng Z, Atanasiu C, Zhao K, Marmorstein R, Sbodio JI, Chi NW, & Lieberman PM (2005). Inhibition of Epstein-Barr virus OriP function by tankyrase, a telomere-associated poly-ADP ribose polymerase that binds and modifies EBNA1. Journal of Virology, 79(8), 4640–4650. 10.1128/jvi.79.8.4640-4650.2005 [PubMed: 15795250]

Egli A, Santer DM, O'Shea D, Tyrrell DL, & Houghton M (2014). The impact of the interferon-lambda family on the innate and adaptive immune response to viral infections. Emerging Microbes & Infections, 3 (7), e51. 10.1038/emi.2014.51 [PubMed: 26038748]

Ehrhardt C, Seyer R, Hrincius ER, Eierhoff T, Wolff T, & Ludwig S (2010). Interplay between influenza a virus and the innate immune signaling. Microbes and Infection, 12, 81–87. 10.1016/j.micinf.2009.09.007 [PubMed: 19782761]

Forster SC, Tate MD, & Hertzog PJ (2015). MicroRNA as type I interferon-regulated transcripts and modulators of the innate immune response. Frontiers in Immunology, 6, 334. 10.3389/fimmu.2015.00334 [PubMed: 26217335]

Garcia-Sastre A (2011). Induction and evasion of type I interferon responses by influenza viruses. Virus Research, 162(1–2), 12–18. 10.1016/j.virusres.2011.10.017 [PubMed: 22027189]

García-Sastre A, Durbin RK, Zheng H, Palese P, Gertner R, Levy DE, & Durbin JE (1998). The role of interferon in influenza virus tissue tropism. Journal of Virology, 72(11), 8550–8558. [PubMed: 9765393]

Gaur P, Munjhal A, & Lal SK (2011). Influenza virus and cell signaling pathways. Medical Science Monitor, 17(6), 148–154 Retrieved from https://www.ncbi.nlm.nih.gov/pmc/articles/PMC3539548/pdf/medscimonit-17-6-ra148.pdf

Goh KC, Haque SJ, & Williams BR (1999). p38 MAP kinase is required for STAT1 serine phosphorylation and transcriptional activation induced by interferons. The EMBO Journal, 18(20), 5601–5608. 10.1093/emboj/18.20.5601 [PubMed: 10523304]

Gui S, Chen X, Zhang M, Zhao F, Wan Y, Wang L, … Liu S (2015). Mir-302c mediates influenza a virus-induced IFNbeta expression by targeting NF-kappaB inducing kinase. FEBS Letters, 589(24 Pt B), 4112–4118. 10.1016/j.febslet.2015.11.011 [PubMed: 26602079]

Guo X.-k., Zhang Q, Gao L, Li N, Chen X.-x., & Feng W.-h. (2013). Increasing expression of MicroRNA 181 inhibits porcine reproductive and respiratory syndrome virus replication and has implications for controlling virus infection. Journal of Virology, 87(2), 1159–1171. 10.1128/jvi.02386-12 [PubMed: 23152505]

He T, Feng G, Chen H, Wang L, & Wang Y (2009). Identification of host encoded microRNAs interacting with novel swine-origin influenza a (H1N1) virus and swine influenza virus. Bioinformation, 4(3), 112–118. [PubMed: 20198183]

Huang C, Xiao X, Yang Y, Mishra A, Liang Y, Zeng X, … Liu L (2017). MicroRNA-101 attenuates pulmonary fibrosis by inhibiting fibroblast proliferation and activation. Journal of Biological Chemistry, 292, 16420–16439. 10.1074/jbc.M117.805747

Huang SM, Mishina YM, Liu S, Cheung A, Stegmeier F, Michaud GA, … Cong F (2009). Tankyrase inhibition stabilizes axin and antagonizes Wnt signalling. Nature, 461(7264), 614–620. 10.1038/nature08356 [PubMed: 19759537]

Hussain M, Galvin HD, Haw TY, Nutsford AN, & Husain M (2017). Drug resistance in influenza a virus: The epidemiology and management. Infection and Drug Resistance, 10, 121–134. 10.2147/IDR.S105473 [PubMed: 28458567]

Ingle H, Kumar S, Raut AA, Mishra A, Kulkarni DD, Kameyama T, … Kumar H (2015). The microRNA miR-485 targets host and influenza virus transcripts to regulate antiviral immunity and restrict viral replication. Science Signaling, 8(406), ra126. 10.1126/scisignal.aab3183 [PubMed: 26645583]

Kaminker PG, Kim SH, Taylor RD, Zebarjadian Y, Funk WD, Morin GB, … Campisi J (2001). TANK2, a new TRF1-associated poly(ADP-ribose) polymerase, causes rapid induction of cell death upon overexpression. The Journal of Biological Chemistry, 276(38), 35891–35899. 10.1074/jbc.M105968200 [PubMed: 11454873]

Kerstin S, Susanna C, Ditte V, Agnieszka P, Solvej ØB, Ralf D, … Peter MHH (2013). Expression of innate immune genes, proteins and microRNAs in lung tissue of pigs infected experimentally with influenza virus (H1N2). Innate Immunity, 19(5), 531–544. 10.1177/1753425912473668 [PubMed: 23405029]

Konig R, Stertz S, Zhou Y, Inoue A, Hoffmann HH, Bhattacharyya S, … Chanda SK (2010). Human host factors required for influenza virus replication. Nature, 463, 813–817. 10.1038/nature08699 [PubMed: 20027183]

Li X, Han H, Zhou M-T, Yang B, Ta AP, Li N, … Wang W (2017). Proteomic analysis of the human tankyrase protein interaction network reveals its role in pexophagy. Cell Reports, 20(3), 737–749. 10.1016/j.celrep.2017.06.077 [PubMed: 28723574]

Li Z, Yamauchi Y, Kamakura M, Murayama T, Goshima F, Kimura H, & Nishiyama Y (2012). Herpes simplex virus requires poly(ADP-ribose) polymerase activity for efficient replication and induces extracellular signal-related kinase-dependent phosphorylation and ICP0-dependent nuclear localization of tankyrase 1. Journal of Virology, 86(1), 492–503. 10.1128/jvi.05897-11 [PubMed: 22013039]

Ludwig S (2009). Targeting cell signalling pathways to fight the flu: Towards a paradigm change in anti-influenza therapy. Journal of Antimicrobial Chemotherapy, 64(1), 1–4. 10.1093/jac/dkp161

Ludwig S, & Planz O (2008). Influenza viruses and the NF-kappaB signaling pathway - towards a novel concept of antiviral therapy. Biological Chemistry, 389(10), 1307–1312. 10.1515/bc.2008.148 [PubMed: 18713017]

Ma G, Wang Y, Li Y, Cui L, Zhao Y, Zhao B, & Li K (2015). MiR-206, a key modulator of skeletal muscle development and disease. International Journal of Biological Sciences, 11(3), 345–352. 10.7150/ijbs.10921 [PubMed: 25678853]

Ma Y-J, Yang J, Fan X-L, Zhao H-B, Hu W, Li Z-P, … Wang S-Q (2012). Cellular microRNA let-7c inhibits M1 protein expression of the H1N1 influenza a virus in infected human lung epithelial cells. Journal of Cellular and Molecular Medicine, 16(10), 2539–2546. 10.1111/j.1582-4934.2012.01572.x [PubMed: 22452878]

More S, Yang X, Zhu Z, Bamunuarachchi G, Guo Y, Huang C, … Liu L (2018). Regulation of influenza virus replication by Wnt/β-catenin signaling. PLoS One, 13(1), e0191010. 10.1371/journal.pone.0191010 [PubMed: 29324866]

Novak J, Kruzliak P, Bienertova-Vasku J, Slaby O, & Novak M (2014). MicroRNA-206: A promising theranostic marker. Theranostics, 4(2), 119–133. 10.7150/thno.7552 [PubMed: 24465270]

Qiu W, Lam R, Voytyuk O, Romanov V, Gordon R, Gebremeskel S, … Chirgadze NY (2014). Insights into the binding of PARP inhibitors to the catalytic domain of human tankyrase-2. Acta Crystallographica. Section D, Biological Crystallography, 70(Pt 10), 2740–2753. 10.1107/s1399004714017660 [PubMed: 25286857]

Reed LJ, & Muench H (1938). A simple method of estimating fifty per cent endpoints12. American Journal of Epidemiology, 27(3), 493–497. 10.1093/oxfordjournals.aje.a118408

Riffell JL, Lord CJ, & Ashworth A (2012). Tankyrase-targeted therapeutics: Expanding opportunities in the PARP family. Nature Reviews. Drug Discovery, 11(12), 923–936. 10.1038/nrd3868 [PubMed: 23197039]

Rolfes MA, F. I, Garg S, Flannery B, Brammer L, Singleton JA, et al. (2016). Estimated Influenza Illnesses, Medical Visits, Hospitalizations, and Deaths Averted by Vaccination in the United States. Retrieved from https://www.cdc.gov/flu/about/disease/2015-16.htm

Rolfes MA, Foppa IM, Garg S, Flannery B, Brammer L, Singleton JA, … Reed C (2018). Annual estimates of the burden of seasonal influenza in the United States: A tool for strengthening influenza surveillance and preparedness. Influenza and Other Respiratory Viruses, 12, (1), 132–137. 10.1111/irv.12486 [PubMed: 29446233]

Roy S, Liu F, & Arav-Boger R (2016). Human cytomegalovirus inhibits the PARsylation activity of Tankyrase—A potential strategy for suppression of the Wnt pathway. Viruses, 8(1), 1–17. 10.3390/v8010008

Sedger LM (2013). microRNA control of interferons and interferon induced anti-viral activity. Molecular Immunology, 56(4), 781–793. 10.1016/j.molimm.2013.07.009 [PubMed: 23962477]

Simon L, Ford SM Jr., Song K, Berner P, Vande Stouwe C, Nelson S, … Molina PE (2017). Decreased myoblast differentiation in chronic binge alcohol-administered simian immunodeficiency virus-infected male macaques: Role of decreased miR-206. American Journal of Physiology. Regulatory, Integrative and Comparative Physiology, 313 (3), R240–r250. 10.1152/ajpregu.00146.2017

Soema PC, Kompier R, Amorij J-P, & Kersten GFA (2015). Current and next generation influenza vaccines: Formulation and production strategies. European Journal of Pharmaceutics and Biopharmaceutics, 94, 251–263. 10.1016/j.ejpb.2015.05.023 [PubMed: 26047796]

Song L, Liu H, Gao S, Jiang W, & Huang W (2010). Cellular microRNAs inhibit replication of the H1N1 influenza a virus in infected cells. Journal of Virology, 84(17), 8849–8860. 10.1128/jvi.00456-10 [PubMed: 20554777]

Tan Y, Lin B, Ye Y, Wen D, Chen L, & Zhou X (2015). Differential expression of serum microRNAs in cirrhosis that evolve into hepatocellular carcinoma related to hepatitis B virus. Oncology Reports, 33(6), 2863–2870. 10.3892/or.2015.3924 [PubMed: 25962820]

Tate MD, Brooks AG, & Reading PC (2008). The role of neutrophils in the upper and lower respiratory tract during influenza virus infection of mice. Respiratory Research, 9, 57. 10.1186/1465-9921-9-57 [PubMed: 18671884]

Taubenberger JK, & Kash JC (2010). Influenza virus evolution, host adaptation, and pandemic formation. Cell Host & Microbe, 7(6), 440–451. 10.1016/j.chom.2010.05.009 [PubMed: 20542248]

Timoneda O, Nunez-Hernandez F, Balcells I, Munoz M, Castello A, Vera G, … Nunez JI (2014). The role of viral and host microRNAs in the Aujeszky's disease virus during the infection process. PLoS One, 9 (1), e86965. 10.1371/journal.pone.0086965 [PubMed: 24475202]

Tripathi S, Batra J, & Lal SK (2015). Interplay between influenza a virus and host factors: Targets for antiviral intervention. Archives of Virology, 160(8), 1877–1891. 10.1007/s00705-015-2452-9 [PubMed: 26016443]

Umbach JL, & Cullen BR (2009). The role of RNAi and microRNAs in animal virus replication and antiviral immunity. Genes & Development, 23(10), 1151–1164. 10.1101/gad.1793309 [PubMed: 19451215]

van de Sandt CE, Kreijtz JHCM, & Rimmelzwaan GF (2012). Evasion of influenza a viruses from innate and adaptive immune responses. Viruses, 4(9), 1438–1476. 10.3390/v4091438 [PubMed: 23170167]

Wack A, Terczynska-Dyla E, & Hartmann R (2015). Guarding the frontiers: The biology of type III interferons. Nature Immunology, 16(8), 802–809. 10.1038/ni.3212 [PubMed: 26194286]

Wang Y, Brahmakshatriya V, Zhu H, Lupiani B, Reddy SM, Yoon B-J, … Zhou H (2009). Identification of differentially expressed miRNAs in chicken lung and trachea with avian influenza virus infection by a deep sequencing approach. BMC Genomics, 10(1), 512. 10.1186/1471-2164-10-512 [PubMed: 19891781]

Yang N (2015). An overview of viral and nonviral delivery systems for microRNA. International Journal of Pharmaceutical Investigation, 5(4), 179–181. 10.4103/2230-973x.167646 [PubMed: 26682187]

Yang X, Zhao C, Bamunuarachchi G, Wang Y, Liang Y, Huang C, … Liu L (2019). miR-193b represses influenza a virus infection by inhibiting Wnt/β-catenin signalling. Cellular Microbiology, 21(5), e13001. 10.1111/cmi.13001 [PubMed: 30650225]

Yoshizawa T, Hammaker D, Sweeney SE, Boyle DL, & Firestein GS (2008). Synoviocyte innate immune responses: I. Differential regulation of interferon responses and the JNK pathway by MAPK kinases. The Journal of Immunology, 181(5), 3252–3258. 10.4049/jimmunol.181.5.3252 [PubMed: 18713996]

Zhang L, Huang C, Guo Y, Gou X, Hinsdale M, Lloyd P, & Liu L (2015). MicroRNA-26b modulates the NF-kappaB pathway in alveolar macrophages by regulating PTEN. Journal of Immunology, 195(11), 5404–5414. 10.4049/jimmunol.1402933

Zhang S, Huo C, Xiao J, Fan T, Zou S, Qi P, … Hu Y (2019). P-STAT1 regulates the influenza a virus replication and inflammatory response in vitro and vivo. Virology, 537, 110–120. 10.1016/j.virol.2019.08.023 [PubMed: 31493649]

Zhao L, Zhu J, Zhou H, Zhao Z, Zou Z, Liu X, … Jin M (2015). Identification of cellular microRNA-136 as a dual regulator of RIG-I-mediated innate immunity that antagonizes H5N1 IAV replication in A549 cells. Scientific Reports, 5, 14991. 10.1038/srep14991 [PubMed: 26450567]

Zhao LJ, Hua X, He SF, Ren H, & Qi ZT (2011). Interferon alpha regulates MAPK and STAT1 pathways in human hepatoma cells. Virology Journal, 8, 157. 10.1186/1743-422x-8-157 [PubMed: 21466707]

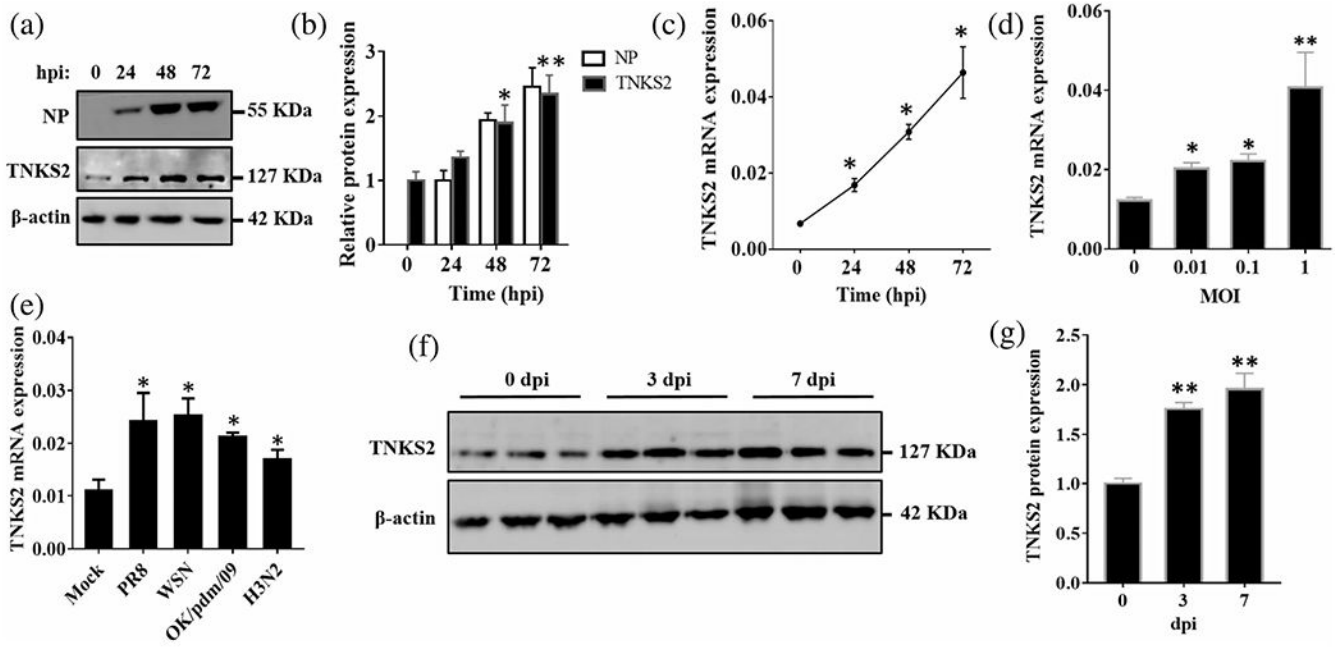

FIGURE 1.

Influenza virus induces TNKS2 expression in vitro and in vivo. (a, b) A549 cells were infected with A/PR/8/34 at an MOI of 0.01 and samples were collected at 0, 24, 48 and 72 hpi. Viral NP and TNKS2 protein levels were determined by western blot and normalised to β-actin ($N = 6$). The results for TNKS2 and NP were expressed as a ratio to 0 and 24 hpi, respectively. (c, d) A549 cells were infected with A/PR/8/34 at an MOI of 0.01 for 0, 24, 48 and 72 hr and different MOI for 24 hr. Relative mRNA expression levels of TNKS2 were measured by real-time PCR and normalised to β-actin ($N = 3$). (e) A549 cells infected with different strains of IAV, including A/PR/8/34, A/WSN/33, pdm/Ok/09, and H3N2 A/OK/309/06, at MOI 0.01 for 48 hpi. Relative mRNA expression levels of TNKS2 were measured by real-time PCR and normalised to β-actin ($N = 3$). (f, g) TNKS2 protein expression in the lungs of mice infected with A/PR/8/34 (250 Pfu) at 3 and 7 days postinfection (dpi) was measured by western blot and expressed as a ratio to 0 dpi ($N = 6$). All results are displayed as the mean ± *SE*. $^{*}p < .05$, $^{**}p < .01$ vs 0 hpi, MOI 0 or Mock. *One-way ANOVA followed by dunnet's pairwise comparison*

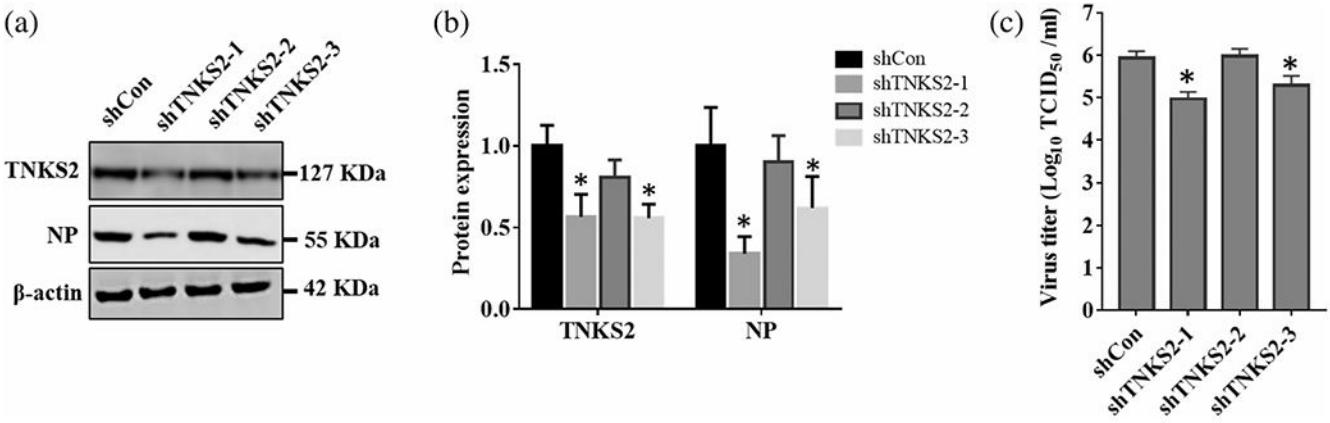

FIGURE 2.

TNKS2 knockdown represses IAV replication. HEK293 cells were transfected with a plasmid expressing TNKS2 shRNA (shTNKS2-1, shTNKS2-2 or shTNKS2-3) or a control plasmid (shCon) and then infected with A/PR/8/34 at an MOI of 0.01 for 48 hr. (a, b) The expression levels of TNKS2 and viral protein (NP) were determined by western blot, normalised to β-actin and expressed as a ratio to shCon. (c) Virus yield in the media was titrated by $TCID_{50}$ assay. Data are expressed as the mean ± *SE* of three independent experiments. $*p < .05$ versus sh-Con (*one-way ANOVA followed by dunnet's pairwise comparison*)

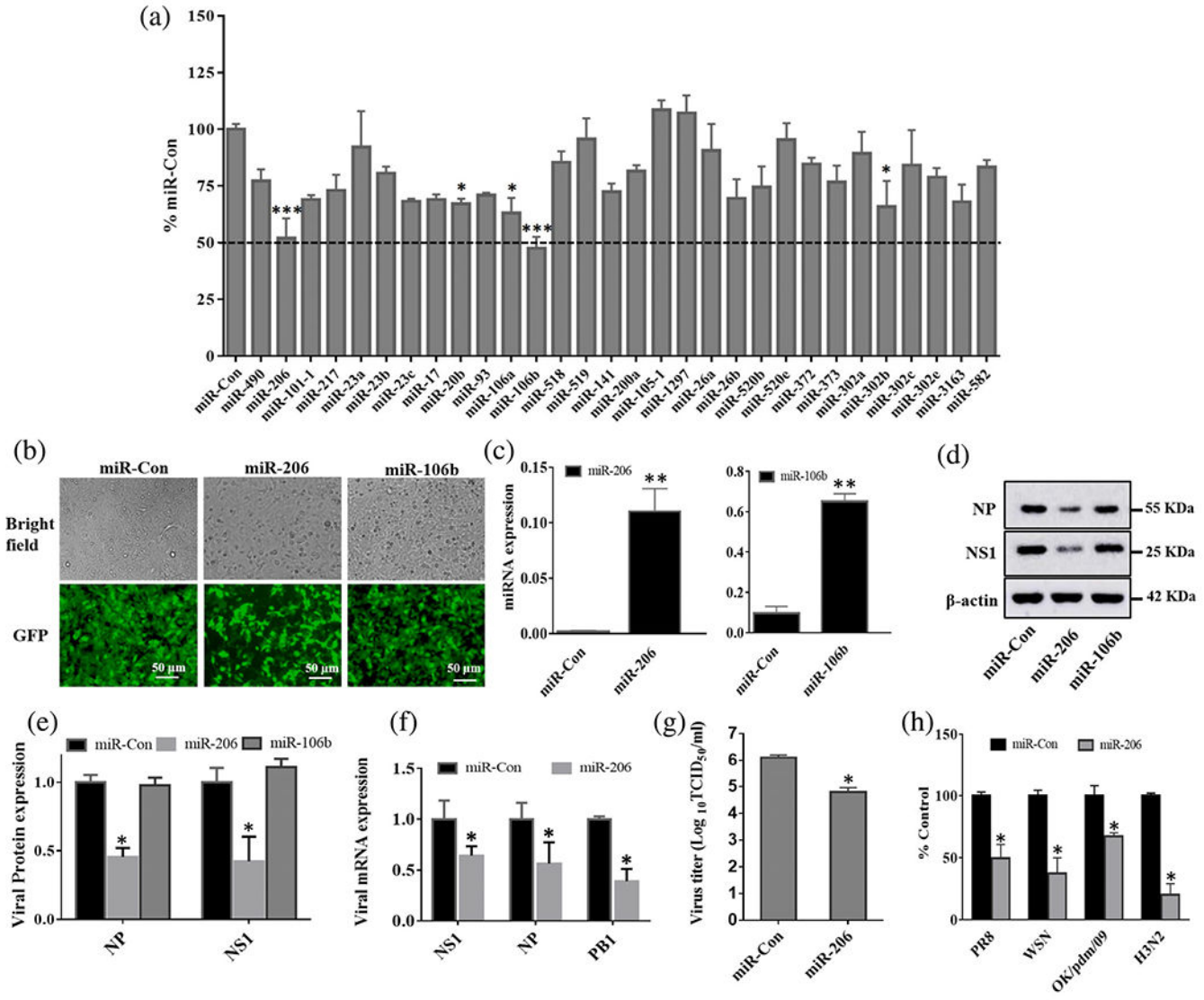

FIGURE 3.

miR-206 inhibits IAV replication. (a) A549 cells were co-transfected with pmirGLO-firefly-TNKS2-3'-UTR reporter plasmid and a miRNA expression plasmid or a miRNA control vector (miR-Con) for 24 hr and luciferase activities were measured. Relative firefly luciferase activities were normalised to *Renilla* luciferase activities and expressed as a percent of miR-Con. (b–g) HEK293 cells were transfected with a miRNA expression vector (miR-206, miR-106b) or a miRNA control vector (miR-Con) for 24 hr. The cells were then infected with A/PR/8/34 virus (MOI = 0.01) for 48 hr. (b) GPF images. (c) Real-time PCR analysis of miRNA expression normalised to U6. (d, e) Viral NP and NS1 protein expression was determined by western blot and normalised to β-actin. (f) mRNA expression of viral genes (NP, NS1, and PB1) was determined by real-time PCR, normalised to β-actin and expressed as a ratio to miR-Con. (g) Virus titers in the culture media were determined by $TCID_{50}$ assay. (h) HEK293 cells were transfected with a miR-206 or miR-Con plasmid (100 ng), the IAV firefly luciferase reporter plasmid vNP-luc/pHH21 (20 ng) and pRL-TK *Renilla*

plasmid (5 ng) for 24 hr. The cells were then infected with different strains of IAV for 48 hr, including A/PR/8/34, A/WSN/33, pdm/Ok/09, and H3N2 A/OK/309/06, at MOI 0.01, 0.05,0.005 and 0.01, respectively. Firefly luciferase activities were normalised to *Renilla* luciferase activity. The results of three independent experiments are displayed as the mean ± *SE*. *$p < .05$, **$p < .01$ vs miR-Con, *Studen's t test* for (c, f, g, h), *One-way ANOVA followed by dunnet's pairwise comparison* for (a), and *two-way ANOVA followed by sidak's pairwise comparison* for (e)

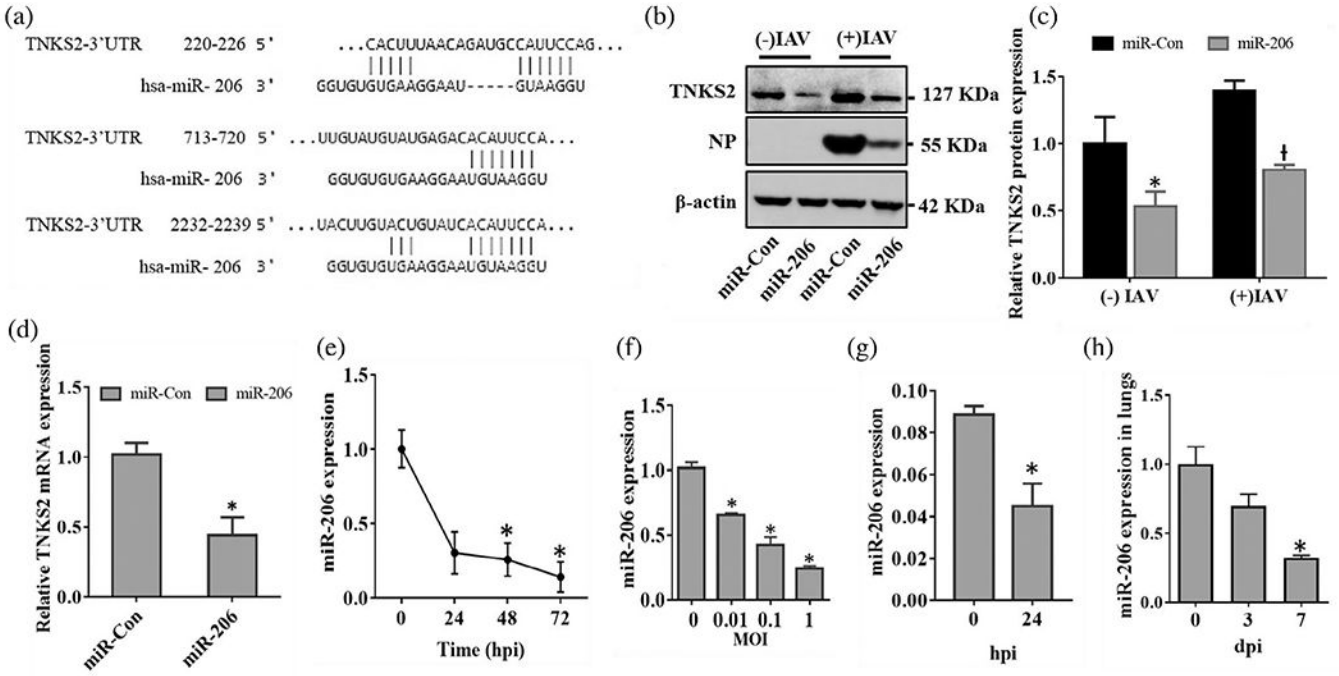

FIGURE 4.

TNKS2 is a target of miR-206 and IAV suppresses endogenous miR-206 expression. (a) Potential interaction between has-miR-206 and the putative binding sites in the 3'-UTR of the human TNKS2 gene. (b–d) A549 cells were infected with miR-206 or miR-Con lentivirus for 24 hr and subsequently infected with or without A/PR/8/34 virus (MOI = 0.01) for 48 hr. TNKS2 and viral NP protein levels were determined by western blot (b, c). TNKS2 mRNA expression without IAV infection was measured by real-time PCR (d). Protein and mRNA levels were normalised to β-actin and expressed as a ratio to miR-Con ($N = 3$). (e, f) A549 cells were infected with A/PR/8/34 either at a MOI of 0.01 for 0, 24, 48 and 72 hr or MOI of 0, 0.01, 0.1, and 1 for 24 hr. (g) HBTEC cells were infected with A/PR/8/34 at a MOI of 0.1 for 24 hr. (h) C57BL/6 mice were infected with 250 pfu A/PR/8/34 for 3 and 7 days. The endogenous miR-206 levels were determined by using real-time PCR, normalised to U6 and expressed as a ratio to non-infected cells (0 hpi) or lungs (0 dpi). $N = 3$ for cells and $N = 6$ for mice. The results are displayed as the mean ± *SE*. *$p < .05$ versus miR-Con, 0 hpi or 0 MOI, *Two-way ANOVA followed by sidak's multiple comparisons* for (c), *Student t test* for (d and g), *and One-way ANOVA followed by dunnet's pairwise comparison* for (e, f and h)

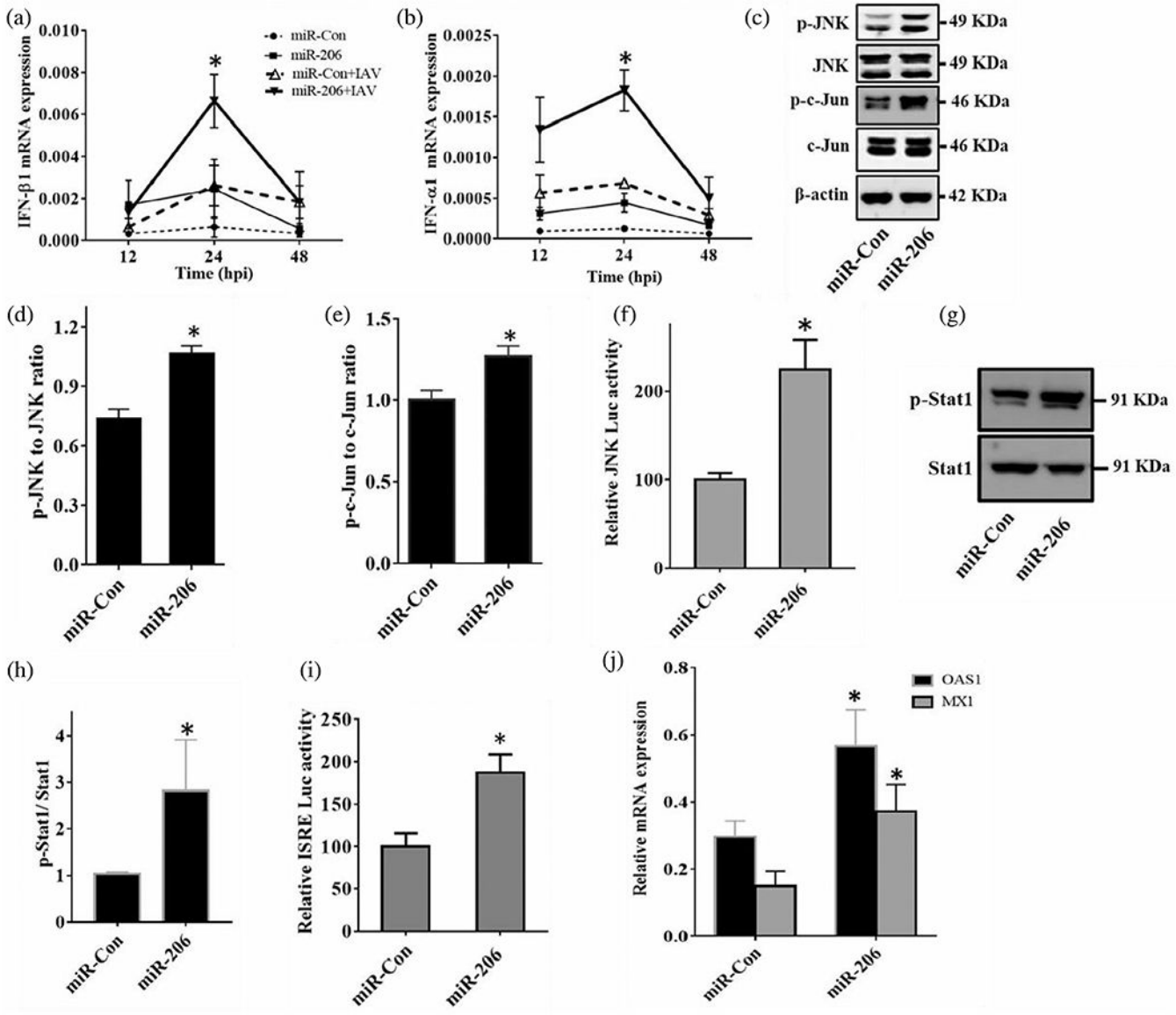

FIGURE 5.

miR-206 activates an anti-viral state in vitro. (a, b) HEK293 were transfected miR-206 expression plasmid or miR-Con for 24 hr and infected with A/PR/8/34 (MOI = 0.01) for 12, 24, and 48 hr. The mRNA expression levels of IFN-β1 and IFN-α1 were determined by realtime PCR and normalised to β-actin. (c–e, g, h) HEK293 cells were transfected with miR-206 or miR-Con expression plasmid for 24 hr and then infected with A/PR/8/34 (MOI = 0.01) for 48 hr. The protein expression levels of p-JNK, p-c-Jun and p-Stat1 were determined by western blot and expressed as a ratio to JNK, c-Jun, and Stat1, respectively. (f, i) HEK293 cells were co-transfected with a miR-con or miR-206 plasmid and a MAPK/JNK Luc vector or ISRE-Luc reporter vector for 24 hr and then infected with A/PR/8/34 (MOI = 0.01) for 48 hr. Luciferase activities were measured and the firefly activities were normalised to *Renilla* luciferase activities. The results were expressed as a percent of miR-Con. (j) HEK293 cells were infected with A/PR/8/34 (MOI = 0.01) for 48 hr.

Relative mRNA expression of OAS1 and Mx1 was measured by real-time PCR and normalised to β-actin. The results of three independent experiments are displayed as the mean ± *SE*. **p* < .05 versus miR-Con at 24 hpi (a, b), Two-way ANOVA *followed by tukey's pairwise comparison*, **p* < .05 versus miR-Con (c–j). *Student t test*

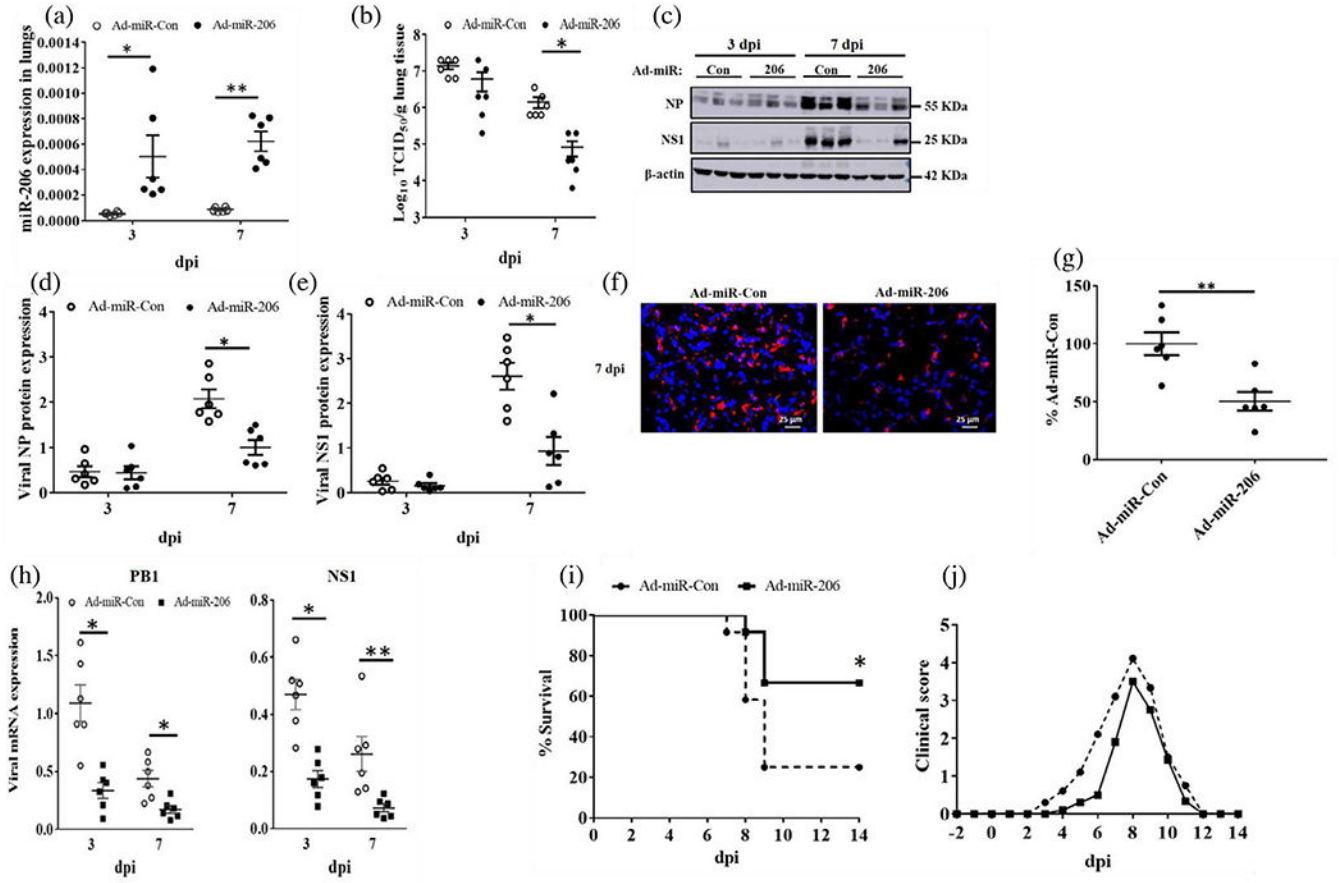

FIGURE 6.

Adenovirus expressing miR-206 suppresses IAV infection in vivo and increases survival of IAV-infected mice. (a–h) Two days before IAV infection (−2 dpi), adenovirus expressing miR-206 (Ad-miR-206) or miR-Con (Ad-miR-Con) was delivered intratracheally into the lungs of mice. The mice were then infected intranasally with a sub-lethal dose (250 PFU/mouse) of A/PR/8/34 on day 0. Lung tissue samples were collected at 3, 7 dpi. (a) miR-206 levels were measured using real-time PCR and normalised to U6 snRNA. (b) The virus titre was determined by $TCID_{50}$ assay. (c–e) Viral NP, NS1 protein levels were determined by western blot, normalised to β-actin. (f, g) Viral replication at 7 dpi in the alveolar regions was determined by immunofluorescent staining for NP. For each section, five pictures were taken randomly from each region with ×20 magnification. Total cells and NP positive cells were counted to determine the percentage of NP positive cells. (h) The mRNA levels of viral NS1 and PB1 mRNA were determined by real-time PCR and normalised to β-actin. The results of six animals are displayed as the mean ± SE. *$p < .05$, ** $p < .01$, (a, b, d, e, h) Two-way ANOVA *followed by sidak's multiple comparisons,* (g) *Student t test.* (i, j) Two days after Ad-miR-206 or Ad-miR-con delivery, mice (N = 12 per group, female) were infected with 1× MLD50 of A/PR/8/34 in 50 μl intranasally. (i) Kaplan-Meier survival analysis of mice. (j) Clinical scores was measured daily. The results were displayed as the mean ± *SE*. *$p < .05$ vs Ad-miR-Con, Mantel-Cox test with Bonferroni-corrected threshold

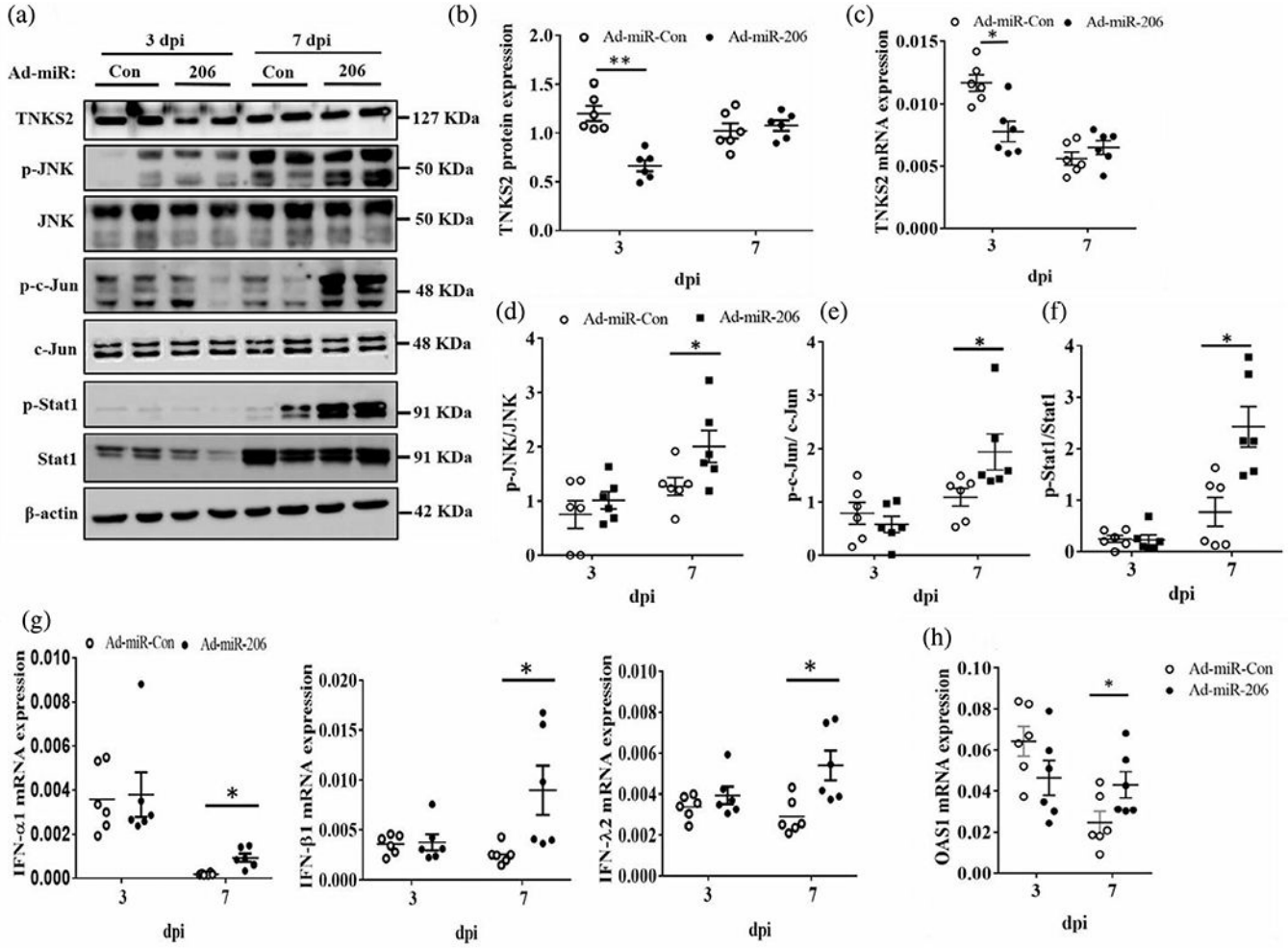

FIGURE 7.

miR-206 activates the anti-viral state in vivo. Two days after miR-206 or miR-con delivery, mice were infected with a sub-lethal dose of A/PR/8/34 (250 PFU/mouse). Lung tissues were collected at 3, 7 dpi. (a) Reprehensive western blots of TNKS2, p-JNK, JNK, p-c-Jun, Jun, p-JAK1, JAK1, p-Stat1, and Stat1. (b) TNKS2 protein levels normalised to β-actin. (c) TNKS2 mRNA levels normalised to β-actin. (d) A ratio of p-JNK to JNK, (e) a ratio of p-c-Jun to Jun. (f) A ratio of p-Stat1 to Stat1. (g) mRNA levels of IFN-α1, IFN-β1, IFN-λ2 normalised to β-actin. (h) OAS1 mRNA levels normalised to β-actin. The results of six animals are displayed as the mean ± *SE*. *$p < .05$ (Two-way ANOVA *followed by sidak's multiple comparisons*)